Front. Electr. Electron. Eng. China 2008, 3(4): 381–387
DOI 10.1007/s11460-008-0086-3

RESEARCH ARTICLE

Ying SUN, Lin WANG, Lei LIU

Integrative decomposition procedure and Kappa statistics set up ATF2 ion binding module in malignant pleural mesothelioma (MPM)

Abstract Activating transcription factor 2 (ATF2) is a member of the ATF/cyclic AMP-responsive element binding protein family of transcription factors. However, the information concerning ATF2 ion-mediated DNA binding module and function of ATF2 in malignant pleural mesothelioma (MPM) has never been addressed. In this study, by using GRNInfer and GVedit based on linear programming and a decomposition procedure, with integrated analysis of the function cluster using Kappa statistics and fuzzy heuristic clustering in MPM, we identified one ATF2 ion-mediated DNA binding module involved in invasive function including ATF2 inhibition to target genes FALZ, C20orf31, NME2, PLOD2, RNF10, and RNASEH1, upstream RNF10 and PLOD2 activation to ATF2, upstream RNASEH1 and FALZ inhibition to ATF2 from 40 MPM tumors and 5 normal pleural tissues. Remarkably, our results showed that the predominant effect of ATF2 occupancy is to suppress the activation of target genes on MPM. Importantly, the ATF2 ion-mediated DNA binding module reflects 'mutual' positive and negative feedback regulation mechanism of ATF2 with up-and down-stream genes. It may be useful for developing novel prognostic markers and therapeutic targets in MPM.

Keywords significant function cluster, inferring analysis, activating transcription factor 2 (ATF2), malignant pleural mesothelioma (MPM)

1 Introduction

Activating transcription factor 2 (ATF2) is a member of the ATF/cyclic AMP-responsive element binding protein family of transcription factors. It has been shown, *in vitro*, to possess growth factor-independent proliferation and transformation capacity [1]. It has been reported that JNK-dependent phosphorylation of ATF2 plays an important role in phenotype drug resistance by mediating enhanced DNA repair by a p53-independent mechanism [2]. Differentiation-dependent expression and phosphorylation of ATF2 protein physically and functionally interacts with C/EBPalpha and coativator ASC-2 and synergizes to induce target gene transcription during granulocytic differentiation [3]. ATF2 and HO-1 are regulated and induced by biliverdin reductase [4]. Human myometrial target genes of the c-Jun NH2-terminal kinase (JNK) pathway affected by ATF2 and ATF2-sm appear to belong to discrete groups [5]. It is also involved in the transcriptional regulation of c-Jun and a number of cell cycle genes, such as cyclin A, cyclin D1, and ATF3 [6–8], as well as the transforming adenovirus protein E1A [9]. Furthermore, Kawasaki et al. reported that ATF2 is a histone acetyltransferase (HAT) that specifically acetylates histones H2B and H4 *in vitro* [10]. Bhoumik et al. concluded that ATF2 specifically recruits MRE11 and NBS1 to DNA repair foci and that the role of ATF2 in DNA damage repair is uncoupled from its transcriptional activity [11]. But the function of ATF2 in tumors still remains as a puzzle. The information concerning ATF2 interaction regulation network and function of ATF2 in malignant pleural mesothelioma (MPM) has never been addressed.

Many researchers studied ion-mediated DNA binding to DNA, such as metal-ion-mediated tuning of duplex DNA binding by bis(2-(2-pyridyl)-1H-benzimidazole), conformational change induced by metal-ion-binding to DNA containing the artificial 1,2,4-triazole nucleoside, preparation and metal ion-binding of 4-N-substituted cytosine pairs off in DNA duplexes [12–14]. However, ion-mediated DNA binding module of ATF2 in MPM is not identified.

In this study, we tried to complement the blank of the implication of ATF2 in MPM. We profiled 40 MPM

Received May 31, 2008; accepted July 4, 2008

Ying SUN, Lin WANG (✉), Lei LIU
Center for Biomedical Engineering, School of Electronics Engineering, Beijing University of Posts and Telecommunications, Beijing 100876, China
E-mail: wanglin98@tsinghua.org.cn

tumors, as well as 5 normal pleural tissues, using microarrays containing 22215 genes to dig the potential function of ATF2 in MPM. In global expression analysis, using the SAM algorithm [15], we identified 51 significant genes with high expression levels that distinguished between normal and MPM tissues. In this study, by using GRNInfer [16] and GVedit (http://www.graphviz.org/) based on linear programming and a decomposition procedure, with integrated analysis of the function cluster using Kappa statistics and fuzzy heuristic clustering in MPM, we identified one ATF2 ion-mediated DNA binding module involved in invasive function including ATF2 inhibition to target genes FALZ, C20orf31, NME2, PLOD2, RNF10, and RNASEH1, upstream RNF10 and PLOD2 activation to ATF2, upstream RNASEH1 and FALZ inhibition to ATF2 from 40 MPM tumors and 5 normal pleural tissues. Remarkably, our results showed that the predominant effect of ATF2 occupancy is to suppress the activation of target genes on MPM. Importantly, The ATF2 ion-mediated DNA binding module reflects "mutual" positive and negative feedback regulation mechanism of ATF2 with up-and down-stream genes. It may be useful for developing novel prognostic markers and therapeutic targets in MPM.

2 Materials and methods

2.1 Microarrays data

In this study, we profiled 40 MPM tumors, as well as 5 normal pleural tissues, using microarrays containing 22215 genes to dig the potential function of ATF2 in MPM from GEO Datasets.

2.2 Gene selection algorithms

Primary data collection and analysis were carried out using SAM. Before that, the expression level of each of the 22215 genes on the microarray was $\log_2$-transformed. SAM is a statistical technique for finding significant genes in a set of microarray experiments. It was proposed by Tusher et al. [15]. The software was written by B. Narasimhan and R. Tibshirani. The input to SAM is gene expression measurements from a set of microarray experiments, as well as a response variable from each experiment. The response variable may be a grouping like untreated, treated (either unpaired or paired), a multiclass grouping (like breast cancer, lymphoma, colon cancer), a quantitative variable (like blood pressure) or a possibly censored survival time. SAM computes a statistic *di* for each gene *i*, measuring the strength of the relationship between gene expression and the response variable. The threshold for significance is determined by a tuning parameter delta. For genes with scores greater than the adjustable threshold, SAM uses repeated permutations of the data to estimate if the expression of any gene is significantly related to the response, the false discovery rate (FDR). One can also choose a fold change parameter to ensure that called genes change at least by a pre-specified amount.

In this study, we chose minimum fold change = 3.5 and delta = 1.59 as the threshold to figure out the potentially significant tumor molecular markers on MPM. By using a two-class-unpaired SAM analysis for comparisons of gene expression levels, we finally selected the top 51 significant positive genes between all 40 tumor samples and all 5 pleura normal samples. The false discovery rate is 0%.

2.3 Network analysis of candidate MPM oncogenes

Network analysis was performed using GRNInfer [16] and GVedit (http://www.graphviz.org/). GRNInfer is the reality of a novel method called gene network reconstruction (GNR) tool, which is based on linear programming and a decomposition procedure, to combine multiple microarray datasets from different conditions for inferring gene regulatory networks. The method theoretically ensures the derivation of the most consistent network structure with respect to all of the datasets, thereby not only significantly alleviating the problem of data scarcity but also remarkably improving the reconstruction reliability.

Generally, a genetic network can be expressed by a set of non-linear differential equations with each gene expression level as variables:

$$\dot{\boldsymbol{x}}(t) = \boldsymbol{f}(\boldsymbol{x}(t)), \tag{1}$$

where $\boldsymbol{x}(t) = (x_1(t), x_2(t), \ldots, x_n(t))^{\mathrm{T}} \in \boldsymbol{R}^n$ and $\boldsymbol{f} = (f_1, f_2, \ldots, f_n)^{\mathrm{T}} : \boldsymbol{R}^n \to \boldsymbol{R}^n$. $x_i(t)$ is the expression level (mRNA concentrations) of gene i at time instance t. Assume that there are a total of m time points for a given experimental condition from microarray, i.e., $t_1, t_2, \ldots, t_m$. f_i is a C^1 class non-linear function.

The linear form of Eq. (1) with appropriate normalization is

$$\dot{\boldsymbol{x}}(t) = \boldsymbol{J}\boldsymbol{x}(t) + \boldsymbol{b}(t),\ t = t_1, t_2, \ldots, t_m, \tag{2}$$

where $\boldsymbol{J} = (J_{ij})_{n \times n} = \partial \boldsymbol{f}(\boldsymbol{x}) / \partial \boldsymbol{x}$ is an $n \times n$ Jacobian matrix or connectivity matrix, and $\boldsymbol{b} = (b_1, b_2, \ldots, b_n)^{\mathrm{T}} \in \boldsymbol{R}^n$ is a vector representing the external stimuli or environment conditions, which is set to zero when there is no external input.

We first adopt the SVD technique to derive a particular solution and simplify the general solution of Eq. (2), using a single time-course dataset. By rewriting Eq. (2), we have

$$\dot{\boldsymbol{X}} = \boldsymbol{J}\boldsymbol{X} + \boldsymbol{B}, \tag{3}$$

where $\boldsymbol{X}=(\boldsymbol{x}(t_1),\boldsymbol{x}(t_2),\ldots,\boldsymbol{x}(t_m))$, $\boldsymbol{B}=(\boldsymbol{b}(t_1),\boldsymbol{b}(t_2),\ldots,\boldsymbol{b}(t_m))$ and $\dot{\boldsymbol{X}}=(\dot{\boldsymbol{x}}(t_1),\dot{\boldsymbol{x}}(t_2),\ldots,\dot{\boldsymbol{x}}(t_m))$ are all $n\times m$ matrices with $\dot{x}_i(t_j)=\left[x_i(t_{j+1})-x_i(t_j)\right]/(t_{j+1}-t_j)$ for $i=1,2,\ldots,n$; $j=1,2,\ldots,m$. By adopting SVD, i.e., $(\boldsymbol{X}^{\mathrm{T}})_{m\times n}=\boldsymbol{U}_{m\times n}\boldsymbol{E}_{n\times n}\boldsymbol{V}^{\mathrm{T}}_{n\times n}$, where $\boldsymbol{U}$ is a unitary $m\times n$ matrix of left eigenvectors, $\boldsymbol{E}=\mathrm{diag}(e_1,e_2,\ldots,e_n)$ is a diagonal $n\times n$ matrix containing the n eigenvalues and $\boldsymbol{V}^{\mathrm{T}}$ is the transpose of a unitary $n\times n$ matrix of right eigenvectors. Without loss of generality, let all non-zero elements of e_k be listed at the end, i.e., $e_1=\cdots=e_i=0$ and $e_{i+1},\ldots,e_n\neq 0$. Then we can have a particular solution with the smallest L_2 norm for the connectivity matrix $\hat{\boldsymbol{J}}=\left(\hat{\boldsymbol{J}}_{ij}\right)_{n\times n}$ as

$$\hat{\boldsymbol{J}}=(\dot{\boldsymbol{X}}-\boldsymbol{B})\boldsymbol{U}\boldsymbol{E}^{-1}\boldsymbol{V}^{\mathrm{T}}, \tag{4}$$

where $\boldsymbol{E}^{-1}=\mathrm{diag}(1/e_i)$ and $1/e_i$ is set to zero if $e_i=0$. Thus, the network family, or the general solution of the connectivity matrix $\boldsymbol{J}=(\boldsymbol{J}_{ij})_{n\times n}$ is

$$\boldsymbol{J}=(\dot{\boldsymbol{X}}-\boldsymbol{B})\boldsymbol{U}\boldsymbol{E}^{-1}\boldsymbol{V}^{\mathrm{T}}+\boldsymbol{Y}\boldsymbol{V}^{\mathrm{T}}=\hat{\boldsymbol{J}}+\boldsymbol{Y}\boldsymbol{V}^{\mathrm{T}}, \tag{5}$$

$\boldsymbol{Y}=(y_{ij})$ is an $n\times n$ matrix, where y_{ij} is zero if $e_j\neq 0$ and is otherwise an arbitrary scalar coefficient. Solutions of Eq. (5) represent all of the possible networks that are consistent with the single microarray dataset, depending on arbitrary $\boldsymbol{Y}$. Notice that $m+1$ points are required in Eq. (5) owing to the estimation of $\dot{\boldsymbol{X}}$.

The 51 significant genes formed a complex network, as shown in Fig. 1. It is displayed graphically as nodes (genes) and edges (the biological relationships between the nodes). The arrow of each edge shows the direction of affection, from the beginning to the end. And the color of an edge reflects the node-to-node relationship (red shows active and blue shows negative). For simplicity, genes are referred to by their symbol. We programmed a new applet by ourselves to select the subnetwork containing ATF2 as well as its related genes from MPM.

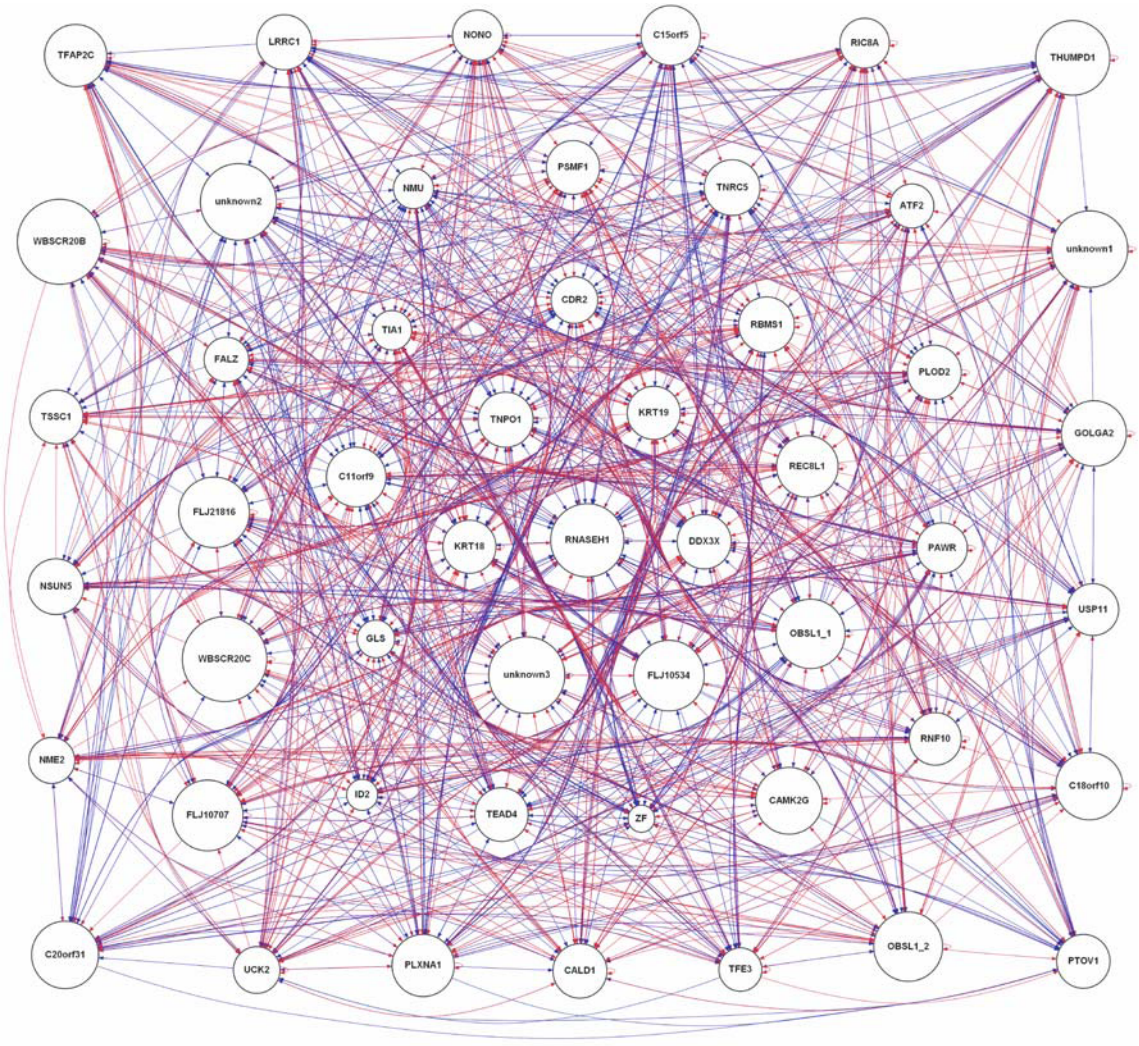

Fig. 1 Network analysis of top 51 significant positive genes

2.4 Functional annotation clustering

Using the function annotation tool of DAVID [17,18], we performed cluster analysis of ATF2 and its related genes. The DAVID functional annotation clustering tool mainly provides typical batch annotation and gene-GO term enrichment analysis to highlight the most relevant GO terms associated with a given gene list. It is a newly-added feature to the DAVID Functional Annotation Tool. This function uses a novel algorithm to measure relationships among the annotation terms based on the degrees of their co-association genes to group the similar, redundant, and heterogeneous annotation contents from the same or different resources into annotation groups. The tool also provides a look at the internal relationships of the clustered terms by comparing it to the typical linear, redundant term report, over which similar annotation terms may be distributed among hundreds or thousands of other terms.

The grouping algorithm is based on the hypothesis that similar annotations should have similar gene members. The Functional Annotation Clustering integrates the same techniques of Kappa statistics to measure the degree of the common genes between two annotations, and fuzzy heuristic clustering (used in Gene Functional Classification Tool) to classify the groups of similar annotations according to the kappa values [18]. In this sense, the more common genes annotations share, the higher chance they will be grouped together.

3 Results

3.1 Identification of MPM tumor molecular markers

We chose minimum fold change = 3.5 and delta = 1.59 as the threshold to figure out the potentially significant tumor molecular markers on MPM. By using a two-class-unpaired SAM analysis for comparisons of gene expression levels, we finally chose the top 51 significant positive genes between all 40 tumor samples and all 5 pleura normal samples with the false discovery rate at 0%. The details of each gene are shown in Table 1. The table does not contain the genes which have turned up more than once, and the ones without any symbol or characterization, which are marked as unknown 1, 2 or 3 in further study.

Table 1 Details of top 51 significant positive genes

gene symbol	gene name
ATF2	activating transcription factor 2
C11orf9	chromosome 11 open reading frame 9
C15orf5	chromosome 15 open reading frame 5
C18orf10	chromosome 18 open reading frame 10
C20orf31	chromosome 20 open reading frame 31
CALD1	caldesmon 1
CAMK2G	calcium/calmodulin-dependent protein kinase (CaM kinase) II gamma
CDR2	cerebellar degeneration-related protein 2, 62 kDa
DDX3X	DEAD (Asp-Glu-Ala-Asp) box polypeptide 3, X-linked
FALZ	fetal Alzheimer antigen
FLJ10534	hypothetical protein FLJ10534
FLJ10707	hypothetical protein FLJ10707
FLJ21816	hypothetical protein FLJ21816
GLS	Glutaminase
GOLGA2	golgi autoantigen, golgin subfamily a, 2
ID2	inhibitor of DNA binding 2, dominant negative helix-loop-helix protein
KRT18	keratin 18
KRT19	keratin 19
LRRC1	leucine rich repeat containing 1
NME2	non-metastatic cells 2, protein (NM23B) expressed in
NMU	neuromedin U
NONO	non-POU domain containing, octamer-binding
NSUN5	NOL1/NOP2/Sun domain family, member 5
OBSL1	obscurin-like 1
PAWR	PRKC, apoptosis, WT1, regulator
PLOD2	procollagen-lysine, 2-oxoglutarate 5-dioxygenase 2
PLXNA1	plexin A1
PSMF1	proteasome (prosome, macropain) inhibitor subunit 1 (PI31)
PTOV1	prostate tumor overexpressed gene 1
RBMS1	RNA binding motif, single stranded interacting protein 1
REC8L1	REC8-like 1 (yeast)
RIC8A	resistance to inhibitors of cholinesterase 8 homolog A (*C. elegans*)
RNASEH1	ribonuclease H1
RNF10	ring finger protein 10
TEAD4	TEA domain family member 4
TFAP2C	transcription factor AP-2 gamma (activating enhancer binding protein 2 gamma)
TFE3	transcription factor binding to IGHM enhancer 3
THUMPD1	THUMP domain containing 1
TIA1	TIA1 cytotoxic granule-associated RNA binding protein
TNPO1	transportin 1
TNRC5	trinucleotide repeat containing 5
TSSC1	tumor suppressing subtransferable candidate 1
UCK2	uridine-cytidine kinase 2
USP11	ubiquitin specific peptidase 11
WBSCR20B	Williams-Beuren Syndrome critical region protein 20 copy B
WBSCR20C	Williams-Beuren Syndrome chromosome region 20C
ZF	HCF-binding transcription factor Zhangfei

3.2 ATF2 functional annotation clustering

We analyzed ATF2 and its related genes were found to be statistically significant in MPM to discover their interactive network relevant to MPM. A gene expression- and interaction-based network of these 51 genes was constructed, using GRNInfer [16] and GVedit (http://www.graphviz.org/), which is based on linear programming and a decomposition procedure. Then we selected the subnetwork containing ATF2 as well as its related genes that are clearly separated into two parts including upstream and target in MPM for further study.

According to ATF2 Functional Annotation Clustering result, one ion-mediated DNA binding module consists

of ATF2 upstream genes including FALZ, PLOD2, RNF10, RNASEH1 as shown in Fig. 2, and the other comprises ATF2 target genes including FALZ, C20orf31, NME2, PLOD2, RNF10, RNASEH1 as shown in Fig. 3.

Fig. 2 Metal ion-binding cluster annotation analysis of ATF2 and its upstream genes including FALZ, PLOD2, RNF10, RNASEH1, using DAVID Function Annotation Clustering tool

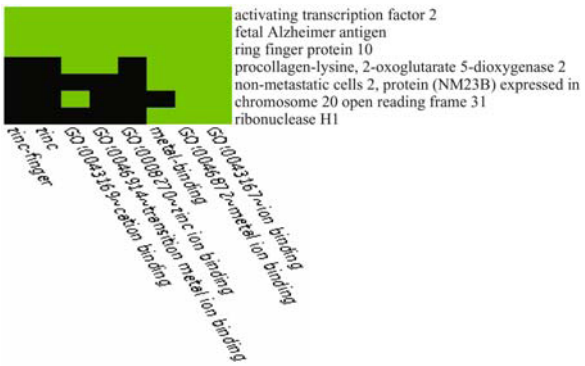

Fig. 3 Metal ion-binding cluster annotation analysis of ATF2 and its target genes including FALZ, C20orf31, NME2, PLOD2, RNF10, RNASEH1, using DAVID Function Annotation Clustering tool

3.3 ATF2 network establishment in MPM

After doing function annotation clustering, we constructed the network of ATF2 and its upstream/target genes in ion-mediated DNA binding cluster separately, using GRNInfer [16] and GVedit (http://www.graphviz.org/), which is based on linear programming and a decomposition procedure, as shown in Fig. 4. ATF2 upstream genes appeared to be the activation to ATF2 including RNF10 and PLOD2 and the inhibition to ATF2 including RNASEH1 and FALZ. ATF2 target genes included the ATF2 inhibition to FALZ, C20orf31, NME2, PLOD2, RNF10, and RNASEH1.

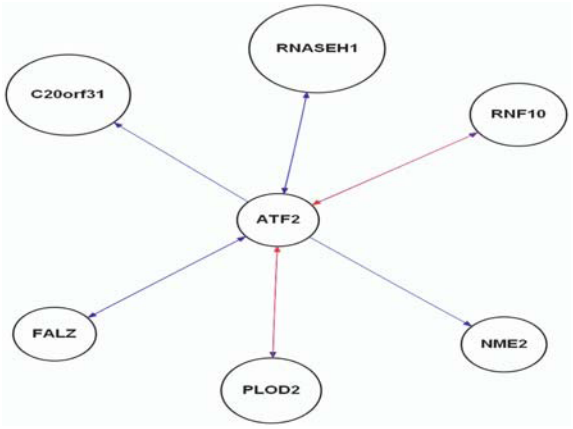

Fig. 4 Network analysis of ATF2 and its upstream/target genes in ion-mediated DNA binding cluster

4 Discussion

ATF2 is a cellular basic region-leucine zipper (bZIP) transcription factor that can mediate diverse transcriptional responses [5]. It has been demonstrated that ATF2 mediates the TGF-beta-induced MMP-2 transcriptional activation, elucidating a molecular mechanism for the malignant progression of human breast epithelial cells exerted by TGF-beta53; it has also been proven that gamma-gene induction by butyrate and trichostatin A involves ATF2 and CREB1 activation via p38 MAPK signaling [19]; in other studies, investigators have found that binding of ATF2 to the CD1A promoter in human monocytes suggests a role for ATF/cAMP response element binding protein family members in regulation of CD1A expression [20]; ATF2 can be activated while resistin induces PTEN expression by activating stress signaling p38 pathway, and in turn induces PTEN expression [21]; p38 MAP kinase-mediated activation of ATF2 was established as a significant mechanism in amylin-evoked beta-cell death, which may serve as a target for pharmaceutical intervention and effective suppression of beta-cell failure in type-2 diabetes [22]; ID2, which can deactivate E2A and perhaps PAX5, is not detectable in normal B cells but is strongly and uniformly expressed in Hodgkin-Reed/Sternberg (HRS) cells of all cases of classical Hodgkin's lymphoma (HL) [23]; OLIG2 expression was predominant over ID2 expression in oligodendroglial tumors, while ID2 expression was predominant over OLIG2 expression in astrocytic tumors [24]; data show that deregulated expression of keratin 18, or an imbalance between keratin 8 and keratin 18, may be an important determinant of Mallory body formation [25]. However, the information concerning ATF2 interaction regulation network and function of ATF2 in MPM has never been addressed. How this transcription factor controls the gene expression programme for MPM is not understood.

In order to predict the potential function of ATF2 in MPM, we performed function cluster analysis of ATF2

upstream and target genes in MPM separately, using functional annotation clustering tool of online DAVID which integrates the same techniques of Kappa statistics to measure the degree of the common genes between two annotations, and fuzzy heuristic clustering to classify the groups of similar annotations according to the kappa values.

Based on integrative significant function cluster and inferring analysis, we identified one ATF2 ion-mediated DNA binding module involved in invasive function is composed of two parts—target genes and upstream genes. ATF2 target genes appeared as ATF2 inhibition to FALZ, C20orf31, NME2, PLOD2, RNF10, RNASEH1, while upstream genes RNF10 and PLOD2 had direct and indirect activation to ATF2, upstream genes RNASEH1 and FALZ inhibition to ATF2, as shown in Fig. 4.

For ATF2 upstream genes appeared PLOD2 activation to ATF2, ATF2 target genes appeared as ATF2 inhibition to PLOD2 from the upper observation. ATF2 upstream genes appeared as RNF10 activation to ATF2, ATF2 target genes appeared as ATF2 inhibition to RNF10 from the upper observation. Therefore, it can be deduced that the relationship of ATF2 with PLOD2 and RNF10 represent negative feedback loop preventing the production of more PLOD2 and RNF10.

ATF2 upstream genes appeared as FALZ and RNASEH1 inhibition to ATF2. ATF2 target genes appeared as ATF2 inhibition to FALZ and RNASEH1 from the upper observation. Therefore, it can be deduced that the relationship of ATF2 with FALZ and RNASEH1 represent positive feedback loop preventing the production of FALZ and RNASEH1.

In this study, by using GRNInfer [16] and GVedit (http://www.graphviz.org/) based on linear programming and a decomposition procedure, with integrated analysis of the function cluster using Kappa statistics and fuzzy heuristic clustering in MPM, we identified one ATF2 ion-mediated DNA binding module involved in invasive function including ATF2 inhibition to target genes FALZ, C20orf31, NME2, PLOD2, RNF10, and RNASEH1, upstream RNF10 and PLOD2 activation to ATF2, upstream RNASEH1 and FALZ inhibition to ATF2 from 40 MPM tumors and 5 normal pleural tissues. Remarkably, our results showed that the predominant effect of ATF2 occupancy is to suppress the activation of target genes on MPM. Importantly, The ATF2 ion-mediated DNA binding module reflects ''mutual'' positive and negative feedback regulation mechanism of ATF2 with up-and down-stream genes. It may be useful for developing novel prognostic markers and therapeutic targets in MPM.

Acknowledgements This work was supported by the National Natural Science Foundation of China (Grant No. 60673109), the Teaching and Scientific Research Foundation for the Returned Overseas Chinese Scholars, Ministry of Education of China.

References

1. Papassava P, Gorgoulis V G, Papaevangeliou D, et al. Overexpression of activating transcription factor-2 is required for tumor growth and progression in mouse skin tumors. Cancer Research, 2004, 64(23): 8573–8584
2. Hayakawa J, Depatie C, Ohmichi M, et al. The activation of c-Jun NH2-terminal kinase (JNK) by DNA-damaging agents serves to promote drug resistance via activating transcription factor 2 (ATF2)-dependent enhanced DNA repair. Journal of Biological Chemistry, 2003, 278(23): 20582–20592
3. Hong S, Choi H M, Park M J, et al. Activation and interaction of ATF2 with the coactivator ASC-2 are responsive for granulocytic differentiation by retinoic acid. Journal of Biological Chemistry, 2004, 279(17): 16996–17003
4. Kravets A, Hu Z, Miralem T, et al. Biliverdin reductase, a novel regulator for induction of activating transcription factor-2 and heme oxygenase-1. Journal of Biological Chemistry, 2004, 279(19): 19916–19923
5. Bailey J, Europe-Finner G N. Identification of human myometrial target genes of the c-Jun NH2-terminal kinase (JNK) pathway: the role of activating transcription factor 2 (ATF2) and a novel spliced isoform ATF2-small. Journal of Molecular Endocrinology, 2005, 34(1): 19–35
6. Shimizu M, Nomura Y, Suzuki H, et al. Activation of the rat cyclin A promoter by ATF2 and Jun family members and its suppression by ATF4. Experimental Cell Research, 1998, 239(1): 93–103
7. Watanabe G, Howe A, Lee R. J, et al. Induction of cyclin D1 by simian virus 40 small tumor antigen. Proceedings of the National Academy of Sciences of the United States of America, 1996, 93(23): 12861–12866
8. Liang G, Wolfgang C D, Chen B P, et al. ATF3 gene. Genomic organization, promoter, and regulation. Journal of Biological Chemistry, 1996, 271(3): 1695–1701
9. Liu F, Green M R. A specific member of the ATF transcription factor family can mediate transcription activation by the adenovirus E1a protein. Cell, 1990, 61(7): 1217–1224
10. Kawasaki H, Schiltz L, Chiu R, et al. ATF-2 has intrinsic histone acetyltransferase activity which is modulated by phosphorylation. Nature, 2000, 405(6783): 195–200
11. Bhoumik A, Takahashi S, Breitweiser W, et al. ATM-dependent phosphorylation of ATF2 is required for the DNA damage response. Molecular Cell, 2005, 18(5): 577–587
12. Bhattacharya S, Chaudhuri P. Metal-ion-mediated tuning of duplex DNA binding by bis(2-(2-pyridyl)-1H-benzimidazole). Chemistry, an Asian Journal, 2007, 2(5): 648–655
13. Böhme D, Düpre N, Megger D A, et al. Conformational change induced by metal-ion-binding to DNA containing the artificial 1,2,4-triazole nucleoside. Inorganic Chemistry, 2007, 46(24): 10114–10119
14. Sugiyama K, Kageyama Y, Okamoto I, et al. Preparation and metal ion-binding of 4-N-substituted cytosine pairs in DNA duplexes. Nucleic Acids Symposium Series (Oxf), 2007, (51): 177–178
15. Tusher V G, Tibshirani R, Chu G. Significance analysis of microarrays applied to the ionizing radiation response. Proceedings of the National Academy of Sciences of the United States of America, 2001, 98(9): 5116–5121
16. Wang Y, Joshi T, Zhang X S, et al. Inferring gene regulatory networks from multiple microarray datasets. Bioinformatics, 2006, 22(19): 2413–2420
17. Dennis G Jr, Sherman B T, Hosack D A, et al. DAVID: database for annotation, visualization, and integrated discovery. Genome Biology, 2003, 4(5): P3

18. Huang da W, Sherman B T, Tan Q, et al. DAVID Bioinformatics Resources: expanded annotation database and novel algorithms to better extract biology from large gene lists. Nucleic Acids Research, 2007, 35(Web Server issue): W169–175
19. Sangerman J, Lee M S, Yao X, et al. Mechanism for fetal hemoglobin induction by histone deacetylase inhibitors involves gamma-globin activation by CREB1 and ATF-2. Blood, 2006, 108(10): 3590–3599
20. Colmone A, Li S, Wang C R. Activating transcription factor/cAMP response element binding protein family member regulated transcription of CD1A. Journal of immunology, 2006, 177(10): 7024–7032
21. Shen Y H, Zhang L, Gan Y, et al. Up-regulation of PTEN (phosphatase and tensin homolog deleted on chromosome ten) mediates p38 MAPK stress signal-induced inhibition of insulin signaling. A cross-talk between stress signaling and insulin signaling in resistin-treated human endothelial cells. Journal of Biological Chemistry, 2006, 281(12): 7727–7736
22. Zhang S, Liu H, Liu J, et al. Activation of activating transcription factor 2 by p38 MAP kinase during apoptosis induced by human amylin in cultured pancreatic beta-cells. FEBS Journal, 2006, 273(16): 3779–3791
23. Renné C, Martin-Subero J I, Eickernjäger M., et al. Aberrant expression of ID2, a suppressor of B-cell-specific gene expression, in Hodgkin's lymphoma. The American Journal of Pathology, 2006, 169(2): 655–664
24. Mikami S, Hirose Y, Yoshida K, et al. Predominant expression of OLIG2 over ID2 in oligodendroglial tumors. Virchows Archiv: an International Journal of Pathology, 2007, 450(5): 575–584
25. Nakamichi I, Hatakeyama S, Nakayama K I. Formation of Mallory body-like inclusions and cell death induced by deregulated expression of keratin 18. Molecular Biology of the Cell, 2002, 13(10): 3441–3451